PERGAMON

International Journal of Heat and Mass Transfer 44 (2001) 587–603

International Journal of HEAT and MASS TRANSFER

www.elsevier.com/locate/ijhmt

A numerical simulation of the convective heat transfer in confined channel flow past square cylinders: comparison of inline and offset tandem pairs

J.L. Rosales[a], A. Ortega[a,*], J.A.C. Humphrey[b]

[a]*Department of Aerospace and Mechanical Engineering, University of Arizona, Tucson AZ 85721, USA*
[b]*College of Engineering, Bucknell University, Lewisburg, PA 17837, USA*

Received 2 July 1999; received in revised form 15 March 2000

Abstract

A numerical investigation was conducted to analyze the unsteady flow-field and heat-transfer characteristics for a tandem pair of square cylinders in a laminar channel flow. The drag, lift, and heat transfer coefficients from the downstream heated cylinder due to inline and offset eddy-promoting cylinders were studied. The results show that the drag coefficient and cylinder Nusselt number decrease as the heated cylinder approaches the wall. The highest Strouhal number value is observed in the channel-centered, inline-eddy configuration. Complex periodic vortex shedding develops when the eddy promoter is offset from the primary cylinder. © 2001 Elsevier Science Ltd. All rights reserved.

1. Introduction

The unsteady, viscous flow past two-dimensional bluff bodies and the resultant vortex shedding have been the focus of numerous numerical and experimental investigations. The motivation behind these studies has been to understand fundamental physics and to find practical applications in industrial processes. These investigations have examined the unsteady nature of the flow behind the bluff bodies and the effects of flow blockage on the heat transfer and Strouhal number. The two-dimensional flow around circular cylinders has been studied in great detail, but recently, rectangular cylinders, flat plates, and other blunt cross-sections have received renewed attention because of their relevance to engineering applications. The motivation behind the current analysis is of a fundamental nature, yet it also relates to the cooling of electronics.

The flow over a three-dimensional bluff object is very different from that of a two-dimensional bluff body and is exceedingly complex, as illustrated by experimental observations [1]. Furthermore, the computing time required to perform a three-dimensional calculation is significantly greater than the time required for a two-dimensional simulation. Therefore, the present investigation is concerned with the two-dimensional, laminar flow and heat transfer for a confined square cylinder with an inline or offset upstream eddy promoter. Despite its geometric simplicity, the fluid flowing past the cylinders displays a complicated unsteady motion and presents an opportunity for understanding basic fluid mechanics that occur in various technologies, especially in the cooling of electronics. An illustration of the two-dimensional geometry of interest is given in Fig. 1. The dynamic

* Corresponding author. Tel.: +1-520-621-6787; fax: +1-520-621-8191.
E-mail address: ortega@u.arizona.edu (A. Ortega).

0017-9310/01/$ - see front matter © 2001 Elsevier Science Ltd. All rights reserved.
PII: S0017-9310(00)00113-7

Nomenclature

- a distance between the top of the heated cylinder and the upper channel wall (m)
- b distance between the top of the eddy-promoting cylinder and the upper channel wall (m)
- c local wave speed in the wave equation (m/s)
- C_D drag coefficient, Eq. (6)
- C_L lift coefficient, Eq. (7)
- d side length of the eddy-promoting cylinder (m)
- D side length of the heated cylinder (m)
- f eddy-shedding frequency from the heated cylinder (s^{-1})
- F_D total force per unit length on the cylinder in the streamwise direction (N/m)
- F_L total force per unit length on the cylinder in the cross-stream direction (N/m)
- h convection heat transfer coefficient, $-k(\partial T/\partial n)_c/(T_c - T_o)$ (W/m^2 K)
- H channel height (m)
- k thermal conductivity (W/m K)
- L distance between the eddy-promoting cylinder back face and the heated cylinder front face (m)
- L_d downstream channel length (m)
- L_u upstream channel length (m)
- n surface normal direction
- Nu Nusselt number, Eq. (5)
- p pressure (Pa)
- Re Reynolds number, UD/ν
- St Strouhal number, fD/U
- t time (s)
- T temperature (K)
- u streamwise velocity (m/s)
- U mean velocity (m/s)
- v cross-stream velocity (m/s)
- x streamwise coordinate direction in Cartesian coordinates (m)
- y cross-stream coordinate direction in Cartesian coordinates (m)

Greek symbols

- α thermal diffusivity of the fluid (m^2/s), or non-dimensional distance between the top of the heated cylinder and the upper channel wall, a/H
- β non-dimensional distance between the top of the eddy-promoting cylinder and the upper channel wall, b/H
- δ size ratio between the eddy-promoting cylinder and the heated cylinder, d/D
- ϕ dependent variable in the wave equation
- λ non-dimensional inter-cylinder spacing, L/D
- ρ density of the fluid (kg/m^3)
- τ time period of oscillation, $1/f$
- ν kinematic viscosity (m^2/s)

Subscripts

- c cylinder value or condition
- m time mean
- o inlet value or condition
- rms root-mean-square of fluctuating component

properties of the present flow were selected to remain below a critical Reynolds number value of 5314, which was calculated as the transition from laminar to turbulent flow in a channel [2]. It has also been reported [3] that flows over square cylinders in channels in the Reynolds number regime of about 500 are laminar to transitional in nature. However, the assumption of laminar flow is not unreasonable since the presence of the channel walls tends to stabilize the flow. The long-range goal of this work is to understand the fundamental mechanisms of unsteady flow interactions in air-cooled channels, beginning with two-dimensional cases, as in the present study, and continuing to three-dimensional situations.

2. Literature review

Earlier numerical studies have investigated the laminar flow past single bluff bodies of square or rectangular cross-section. However, the flow past tandem square cylinders has not yet been studied in great detail. Tandem cylinder arrangements are of fundamental interest and can provide information for practical applications. Tatsutani, et al. [4] studied tandem square cylinders in a channel for Reynolds numbers between 200 and 1,600 based on the downstream cylinder. They observed distinct flow patterns that are dependent on a critical inter-cylinder spacing, λ_c, given by $\lambda_c = 168 \cdot Re^{-2/3}$. Below the critical spacing, two counter-rotating eddies formed in the gap between the square cylinders and vortex shedding was only observed for the downstream cylinder. At the critical spacing, eddy shedding was initiated for the upstream square cylinder. A reduction in the size of the eddy promoter caused an increase in the frequency of eddy shedding from the downstream square cylinder. In a similar numerical study, Valencia [5] investigated the separation distances using equally sized rectangular cylinders. He observed that the channel blockage ratio

was the dominant parameter for heat-transfer enhancement. Devarakonda and Humphrey [6] performed experimental and numerical investigations for the unsteady flow past a tandem pair of square cylinders for a Reynolds number of 592 based on the downstream cylinder. The presence of an eddy promoter enhanced the heat transfer of the downstream cylinder and reduced the drag experienced by the two cylinders. The channel flow had a uniform inlet profile. Subsequently, Devarakonda [7] numerically showed that the heat transfer from the downstream cylinder was maximized for certain inter-cylinder separations. Configurations that yielded a negative or zero drag coefficient for the downstream square cylinder were also found. A comprehensive review of earlier work on single rectangular cylinders is available in Rosales et al. [8].

3. Objectives of this study

From a review of the literature, it is evident that not much work has been done in the area of tandem bluff bodies. An investigation by Rosales et al. [8] has demonstrated that an upstream eddy promoter causes significant changes in the shedding frequency of the primary cylinder as well as in the drag coefficient. Furthermore, it has been shown that interesting flow patterns result from the placement of tandem cylinders near a wall. It is apparent that no systematic study for offset eddy promoters has been considered. The main objective of this investigation has been to perform numerical calculations to understand the effects of the cylinder arrangements on aerodynamic and heat-transfer values for forced convection in a channel. The main issues motivating the present study are: (i) how do offset tandem pairs compare to inline tandem configurations in heat transfer removal? (ii) how does the presence of the wall affect the flow and heat transfer for the offset configuration? (iii) is the flow unsteadiness altered considerably by offsetting the eddy promoter? The present research seeks to clarify these questions while recognizing that our study is only a partial contribution to a larger systematic investigation. It is our goal to have a better understanding of the unsteady flow dynamics driven by the vortex shedding phenomenon.

4. Numerical method

An incompressible finite-volume computer program,

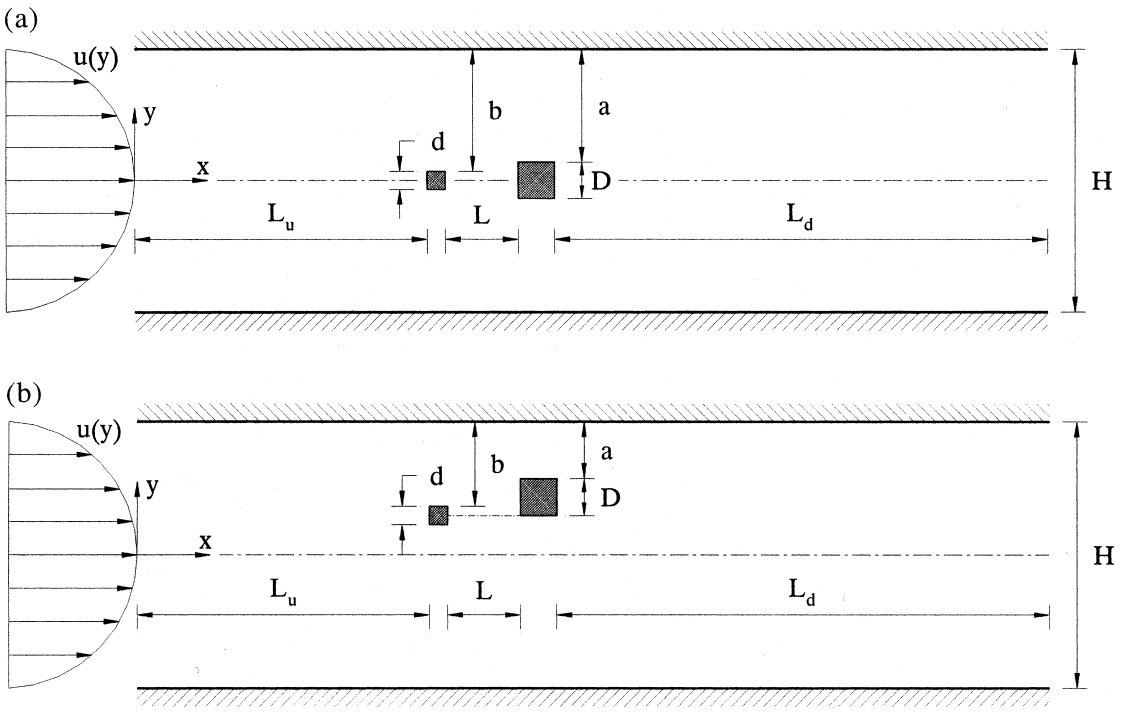

Fig. 1. (a) Schematic of an inline tandem pair of square cylinders in a channel. (b) Schematic of an offset tandem pair of square cylinders in a channel.

FAHTSO (Fluid And Heat Transfer SOlver), was used to perform the numerical calculations. The program is a custom CFD/CHT solver based on the work of Queipo et al. [9,10] and is described in detail by Rosales [11]. The code has been further developed to solve two- or three-dimensional, steady or unsteady laminar flows using the SIMPLE (Semi-Implicit Method for Pressure Linked Equations) algorithm described by Patankar [12]. The program is based on the derivation of the discretized governing equations using the staggered grid, control-volume formulation. The modified strongly implicit procedure [13] was used to solve the system of algebraic equations. The convection terms were discretized using a third-order QUICK scheme while the diffusion terms were discretized using second-order, central differencing. A fully implicit, second-order three-level time scheme is used to solve the time-dependent equations.

5. Governing equations

The flow is assumed to be unsteady, two-dimensional, non-isothermal, and laminar, and the fluid is assumed to be Newtonian with constant properties. The relevant conservation equations describing the flow are continuity, and time-dependent Navier–Stokes and energy equations.

$$\nabla \cdot \vec{u} = 0 \tag{1}$$

$$\frac{\partial \vec{u}}{\partial t} + \vec{u} \cdot \nabla \vec{u} = -\frac{1}{\rho}\nabla p + \nu \nabla^2 \vec{u} \tag{2}$$

$$\frac{\partial T}{\partial t} + \vec{u} \cdot \nabla T = \alpha \nabla^2 T \tag{3}$$

In these equations, ρ is the density; ν is the kinematic viscosity; and α is the thermal diffusivity of the fluid. The velocity vector is represented by $\vec{u}$, p is pressure, T is temperature and t is time. The numerical procedure solves the equations in terms of the primitive variables, velocity, pressure and temperature on a non-uniform, staggered grid.

The geometry studied is shown schematically in Fig. 1. The dimensional values for the heated cylinder diameter, D, and the eddy promoter diameter, d, are 0.01 and 0.005 m, respectively, with a fixed inter-cylinder spacing, L, of 0.02 m. The channel height, H, is 0.0727 m with an overall channel length of 0.355 m. The distance between the inlet plane and the front face of the upstream cylinder, L_u, is 0.08 m, and the distance between the back face of the downstream cylinder and the channel exit plane, L_d, is 0.24 m. A fully developed velocity profile with an average value of 0.7875 m/s is prescribed at the inlet such that the cylinder Reynolds number is 500 based on the side length, D, and the channel Reynolds number is 3635 based on its height, H. A uniform temperature, T_o, is fixed at the inlet plane. The downstream cylinder is placed at a fixed distance downstream of the inlet plane as shown in Figs. 1(a) and (b) and held at a constant temperature T_c. No-slip, impermeable boundary conditions for the velocity are imposed on the upper and the lower channel walls and on the cylinders. The walls are specified as adiabatic, as is the upstream eddy promoter. The exit boundary conditions are chosen to minimize the distortion of the unsteady vortices shed from the cylinders and to reduce perturbations that reflect back into the domain.

A detailed investigation found that the wave equation was the most computationally efficient mathematical condition compatible with the physics at the exit plane, i.e.

$$\frac{\partial \phi}{\partial t} + c\frac{\partial \phi}{\partial x} = 0 \tag{4}$$

where the variable ϕ is the independent variable u, v, or T. Eq. (4) is enforced at the exit plane for the momentum and energy equations, Eqs. (2) and (3). The wave speed, c, is the mean-channel, inlet velocity, U_o. A comprehensive study of the exit plane boundary conditions that were investigated is provided in Rosales et al. [8]. An extensive grid and time-step analysis was performed to correctly capture the highly unsteady flow features present in these laminar channel flow calculations. An examination of the time means for parameters such as the lift and drag coefficients and the Nusselt number, and their rms deviation, indicated that a grid of 188 × 114 and a time step of $0.125E$–03 s were adequate for the simulation of these flows. A sample grid for an offset pair of cylinders in a channel consisting of 188 × 114 internal control nodes

Table 1
Summary of test cases calculated

α (a/H)	β (b/H)	δ (d/D)	λ (L/D)	Re_D
Inline tandem cylinders				
0.431	0.466	0.5	2.0	500
0.216	0.250	0.5	2.0	500
0.108	0.142	0.5	2.0	500
Offset tandem cylinders				
0.431	0.397	0.5	2.0	500
0.216	0.319	0.5	2.0	500
0.216	0.181	0.5	2.0	500
0.108	0.211	0.5	2.0	500
0.108	0.0734	0.5	2.0	500

is shown in Fig. 2. A detailed study is provided in Rosales [11].

All numerical calculations were performed on an SGI Origin2000 system at the University of Arizona. The actual CPU time was not determined for any of the simulations.

6. Results and discussion

Numerical calculations were performed for eight cases which are summarized in Table 1. The heated square cylinder was placed at the center of the channel and at two locations approaching the wall. The eddy-promoting cylinder was placed either inline with the primary cylinder or it was offset and centered on the upper or lower edges of the heated cylinder. Because of symmetry, when the heated cylinder is centered in the channel, the eddy promoter is only offset to one edge of the primary cylinder. All the simulations were performed for a fixed cylinder Reynolds number of 500 and a fixed inter-cylinder spacing, $L/D = 2.0$.

The instantaneous values of the drag and lift coefficients and the Nusselt number on the heated cylinder were calculated at each time step and plotted versus time. The time-averaged values of these parameters were also determined for each case. The time histories for the drag and lift coefficients were used to determine the eddy-shedding frequency. One eddy-shedding cycle is composed of a pair of opposite signed vortices being shed from the downstream cylinder. A Fourier transform was performed on the time series of these quantities to determine the eddy-shedding Strouhal number. The average Nusselt number for each surface of the heated cylinder as well as the total average cylinder Nusselt number were found. The Nusselt number is defined in this study as:

$$Nu = \frac{hD}{k} \tag{5}$$

where h is the heat transfer coefficient and k is the thermal conductivity of the fluid. The viscous and pressure forces acting on the cylinder were used to calculate the drag and lift coefficients. The drag and lift coefficients are defined as:

$$C_{\mathrm{D}} = \frac{F_D}{\frac{1}{2}\rho U_{\mathrm{o}}^2 D} \tag{6}$$

$$C_{\mathrm{L}} = \frac{F_L}{\frac{1}{2}\rho U_{\mathrm{o}}^2 D} \tag{7}$$

where F_{D} and F_{L} are the drag and lift forces exerted by the fluid on the cylinder, respectively. These forces are calculated by integrating the pressure and viscous shear forces over the surface of the cylinder. The drag and lift due to viscous stresses were observed to be small in comparison to the drag and lift due to the pressure forces.

7. Inline tandem arrangement

Rosales et al. [8] conducted a numerical investigation for single and inline tandem square cylinders located in a channel with a parabolic inlet velocity profile. They observed that the cylinder Nusselt number was slightly larger for the tandem pair and decreased as the heated cylinder approached the channel wall. The Strouhal number increased from 0.242 for the channel-centered single cylinder to 0.357 for the channel-centered tandem configuration with the same inter-cylinder spacing as the present study. Conversely, for the same arrangement, the drag coefficient decreased from 4.88 for the single cylinder to 1.33 for the larger cylinder in the tandem pair configuration. The dominant effect observed is the deflection of the flow by the eddy promoter around the primary cylinder, which helps to reduce the force acting on the front face of the heated cylinder. Figs. 3 and 4 show time-series snapshots and temporal traces of the unsteady drag and lift coefficients, respectively, for the tandem cylinders for $\alpha = 0.431$. A pair of bound vortices develops between the two cylinders that exhibits an asymmetric pattern, as shown in Fig. 3. This uneven behavior results in an

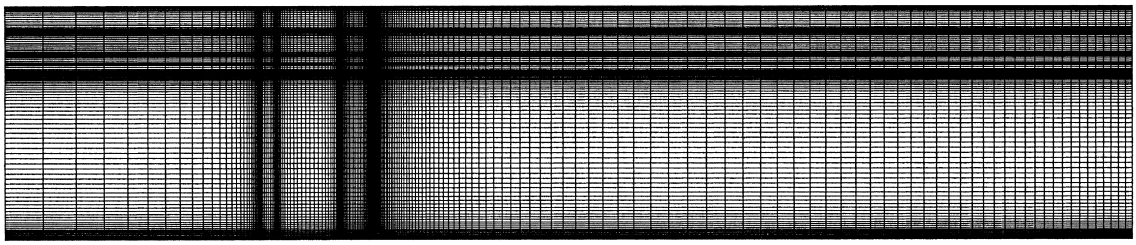

Fig. 2. Non-uniform grid structure for the offset tandem cylinders ($\alpha = 0.108$, $\beta = 0.211$).

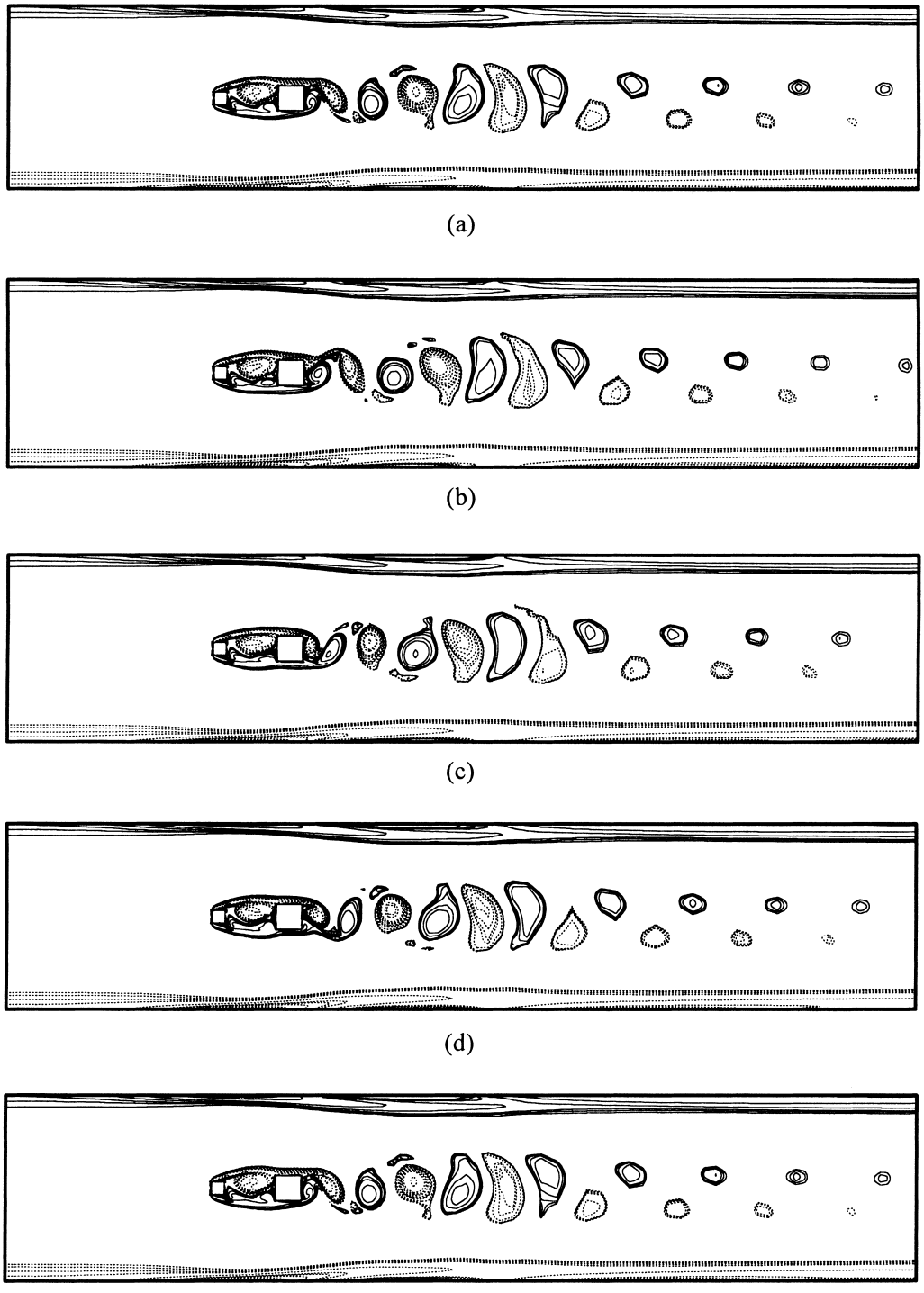

Fig. 3. Time series of vorticity for inline tandem cylinders ($\alpha = 0.431$, $\beta = 0.466$); (a) $\tau = 0$, (b) $\tau = 0.25$, (c) $\tau = 0.50$, (d) $\tau = 0.75$, (e) $\tau = 1.0$.

asymmetry in the lift coefficient and in a larger Nusselt number value on the bottom face of the heated cylinder than on the top face. Fig. 4 reveals that the drag coefficient oscillates at twice the frequency of the lift coefficient. Furthermore, a phase shift is present in the peak values of the curves for the drag and lift coefficients. The asymmetric condition is also evident in the drag coefficient curve as an alternating high and low peak to peak value. Figs. 5 and 6 illustrate time-series snapshots and temporal traces of the unsteady drag and lift coefficients, respectively, for the tandem cylinders for $\alpha = 0.108$. In contrast to the channel-centered configuration, vortex shedding from the eddy promoter is observable. In the channel-centered configuration, the vortex pair is stretched and not allowed to separate because of the presence of the downstream, heated cylinder. Due to the lower velocity fluid near the wall, the vortices are not stretched as intensely, allowing them to form, separate, and shed from the eddy promoter. When the heated cylinder is placed near the wall, the front surface experiences a higher heat transfer rate than when centered in the channel because of flow unsteadiness caused by the alternate sweeping of the vortices on the front face of the primary cylinder. Close observation of Fig. 5(a) reveals that the vortices exiting the channel are formed only on the lower surfaces of the cylinders (Fig. 5a). The presence of the eddy promoter also helps to channel the flow between the upper surface of the downstream cylinder and the wall, which causes the fluid to accelerate in the narrow gap as observed in plots of the streamlines. An earlier study with a single cylinder in a channel [8] found that the vortex separating from the lower surface of the heated cylinder sweeps towards the wall and shuts off the flow jetting in from the narrow space between the cylinder and the wall. In the present case, however, there is a continuous flow of fluid in the narrow gap between the cylinder and the wall that distorts the vortex forming on the lower surface of the primary cylinder. As a vortex separates from the lower surface of the heated cylinder, it coalesces with a vortex shed from the lower surface of the upstream eddy promoter and is advected downstream with remarkable coherence. The vortex circulation on the lower surface of the cylinder is counter-clockwise due to the shear of the main flow below the cylinder. Fig. 6 shows that the shedding cycle for the drag coefficient is almost the same as the shedding cycle for the lift coefficient because vortex shedding from the upper surface is almost completely suppressed. A close examination of Fig. 5 reveals that the vortices that emerge from the narrow gap between the primary cylinder and the wall emanate from the upstream, eddy promoter.

The amplitude of the eddy-shedding oscillations

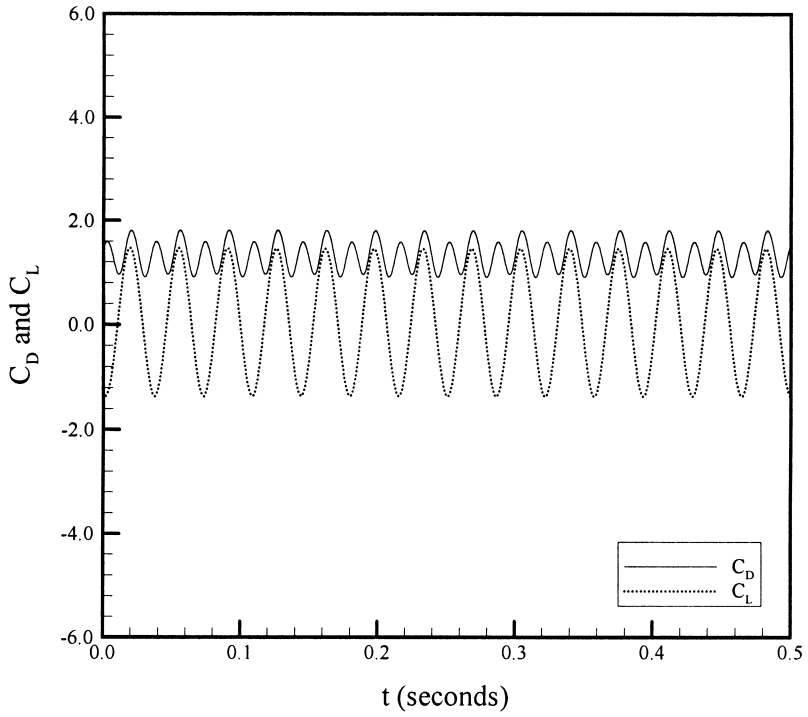

Fig. 4. Instantaneous drag and lift coefficients for the inline cylinders ($\alpha = 0.431$, $\beta = 0.466$).

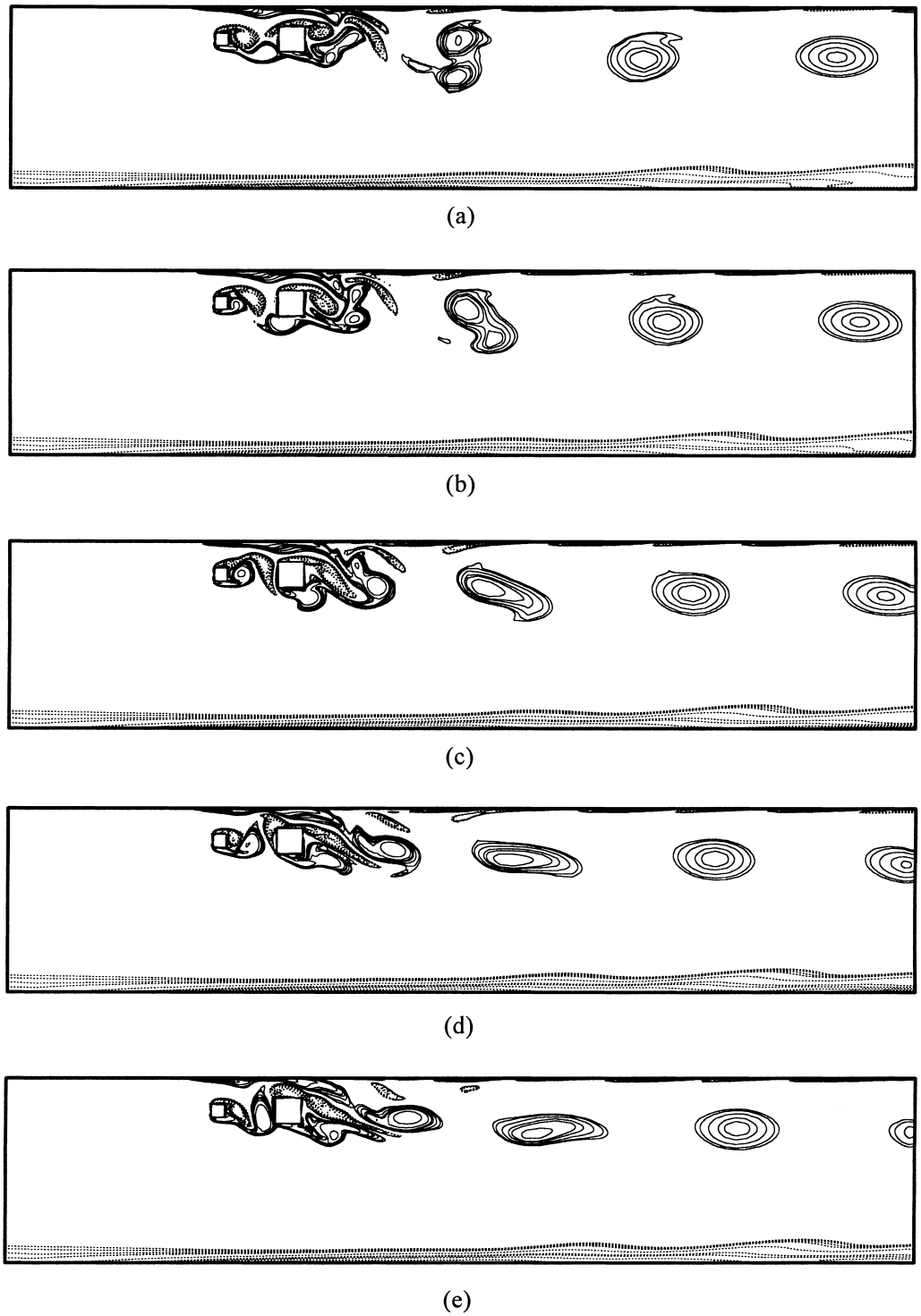

Fig. 5. Time series of velocity for inline tandem cylinders ($\alpha = 0.108$, $\beta = 0.142$): (a) $\tau = 0$, (b) $\tau = 0.25$, (c) $\tau = 0.50$, (d) $\tau = 0.75$, (e) $\tau = 1.0$.

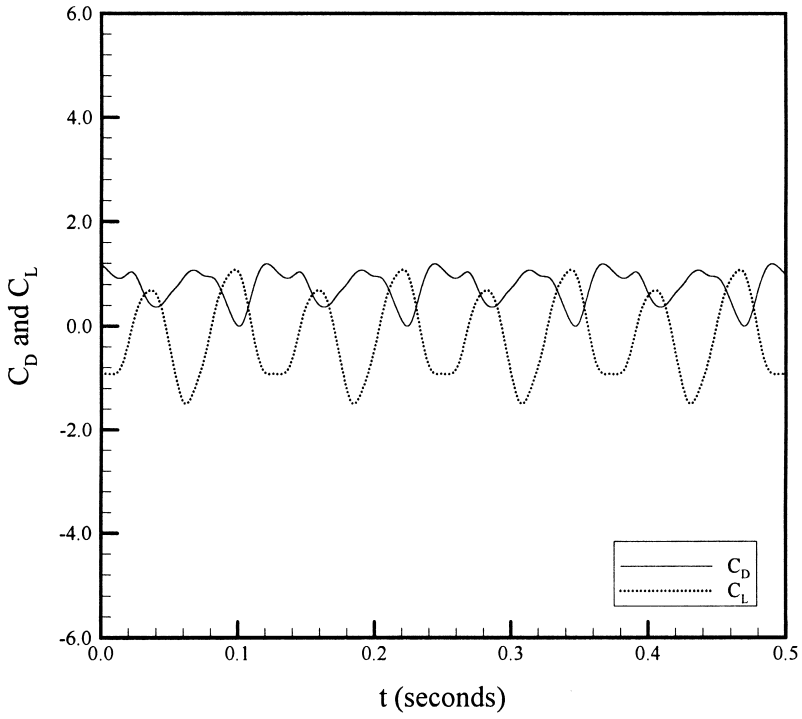

Fig. 6. Instantaneous drag and lift coefficients for the inline cylinders ($\alpha = 0.108$, $\beta = 0.142$).

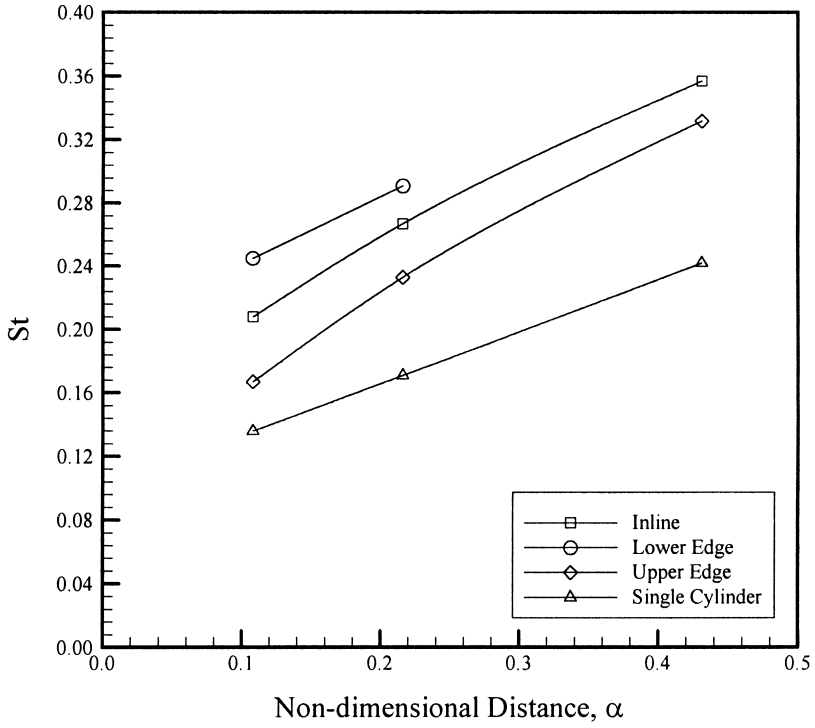

Fig. 7. Strouhal number as a function of position for the inline and offset tandem cylinders.

increases appreciably when the cylinders are moved off-center and then decreases as the wall is approached. This behavior can be observed in the unsteady lift coefficient, C_L, whose RMS value increases from 0.994 to 1.90 when moved off-center and then decreases to a value of 0.778 near the wall. Fig. 7 shows that the Strouhal number decreases as the tandem cylinders approach the wall. The front face of the heated cylinder has the highest surface-averaged Nusselt number value, except when the cylinders are centered in the channel, followed by the bottom, top and rear faces, as shown in Fig. 8. In the centered position, the separated flow from the upstream eddy promoter reattaches on the top and bottom surfaces of the heated cylinder. This causes the time-averaged Nusselt numbers on the side faces to be higher than the front face. When displaced from the center of the channel, the separated flow is allowed to reattach on the front cylinder surface. The displacement of the cylinders into lower velocity fluid causes a net decrease in the overall heat transfer from the heated cylinder as the wall is approached, as seen in Fig. 9. As cited earlier, the increased flow unsteadiness enhances the heat transfer from the front surface of the heated cylinder, but it cannot compensate for a decreased mean velocity, which results in a reduction in the heat transfer from the bottom, top, and rear surfaces. Not surprisingly the cylinder drag, C_D, drops as well, as shown in Fig. 10. In a previous study [8], an examination of Fig. 8 showed an interesting difference between the values of the time-averaged Nusselt number for the top and bottom faces for the inline, channel-centered position. A careful study, to be reported elsewhere, revealed that the Nusselt number values on the top and bottom surfaces could switch, depending on how the flow was initiated, leading to a hypothesis that an asymmetric solution exists due to a bifurcation in the flow.

8. Offset tandem arrangement

Devarakonda [7] calculated the case of an offset tandem pair of square cylinders exposed to a uniform inlet velocity profile for $\lambda = 3.0$ and observed that the Strouhal number was larger than for an inline pair of cylinders. The time-averaged Nusselt number as well as the drag coefficient was insensitive to the staggered arrangement and the values were similar to those for a single cylinder. In the present case, with a parabolic velocity profile the effects are more complex and the results are markedly different.

When the heated cylinder is centered in the channel, moving the eddy promoter from an inline to a stag-

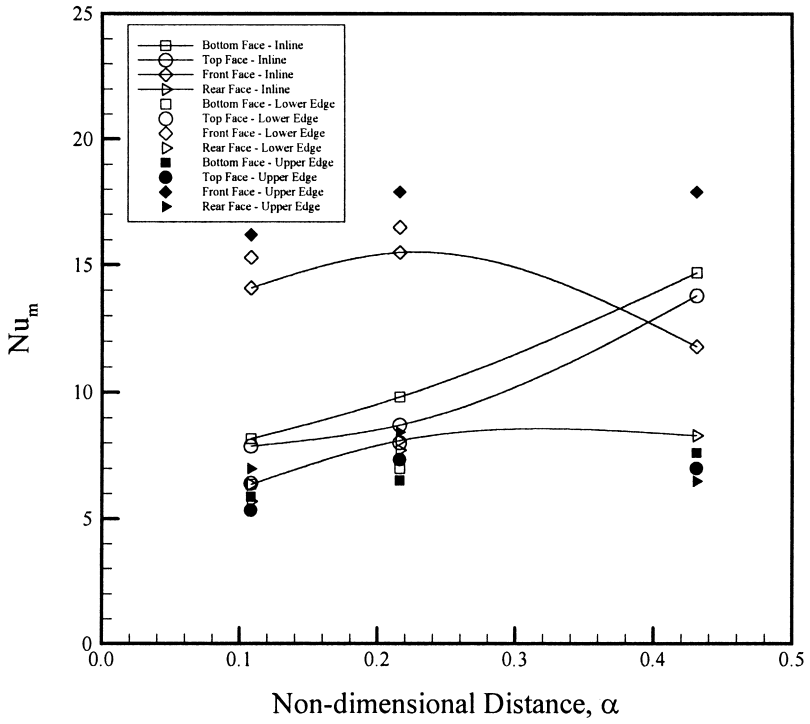

Fig. 8. Time-averaged Nusselt number as a function of cylinder position in the channel for each face of the heated cylinder.

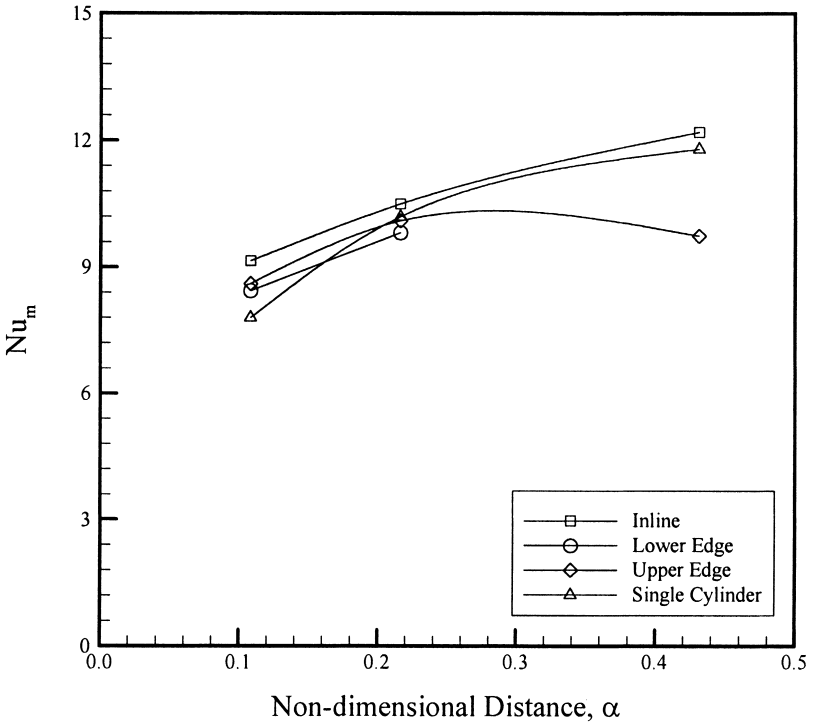

Fig. 9. Time-averaged Nusselt number as a function of cylinder position in the channel for the heated cylinder.

gered position decreases the Strouhal number as shown in Fig. 7. When the heated cylinder is placed at $\alpha = 0.216$ and $\alpha = 0.108$, staggering the eddy promoter to the lower edge of the primary cylinder increases the Strouhal number when compared to the inline configuration. For the same primary cylinder locations, staggering the eddy cylinder to the upper edge of the primary cylinder always gives the lowest Strouhal number values. It has been observed that the downstream heated cylinder locks on to the eddy-shedding frequency of the eddy promoter. This causes both cylinders to shed at the same frequency. For the channel-centered, heated cylinder with an offset eddy promoter, traces of the lift oscillations for both cylinders are shifted in phase by about 20% with the eddy cylinder lift trace leading the primary cylinder lift trace, as shown in Fig. 11. The shedding frequency of the eddy promoter depends upon the local velocity, and therefore, on its location in the channel. When the heated cylinder is centered in the channel, the inline configuration places the eddy promoter in a location where it can experience the highest possible approach velocity. The largest value for the Strouhal number of 0.357 is observed for this location. When the eddy promoter is staggered and placed in a lower velocity fluid, the Strouhal number decreases to 0.332. The placement of the heated cylinder off-center causes the eddy promoter to encounter a different approach velocity for all positions. For $\alpha = 0.216$, the value of the Strouhal number is 0.291, 0.267 and 0.233 when the eddy promoter is located at the lower edge, inline and the upper edge, respectively. In a parabolic flow, the lower edge experiences the highest approach velocity followed by the inline and upper edge. This behavior of the Strouhal number is also observed when the heated cylinder is located at $\alpha = 0.108$.

Fig. 9 compares the values of the time-averaged Nusselt number as a function of position for both inline and offset cylinder configurations. For a fully-developed inlet velocity profile, the inline configuration consistently displays the highest Nusselt number value. Although heat transfer on the front surface of the heated cylinder is increased for the staggered configurations, it does not compensate for the decrease in heat transfer observed on the side and rear faces, as shown in Fig. 8. The time-averaged drag on the primary cylinder differs slightly when the eddy promoter is staggered to either edge, as shown in Fig. 10. The inline configuration always displays the lowest drag and approaches the values of the staggered arrangements as the wall is approached. Figs. 12 and 13 show time-series snapshots and temporal traces of the unsteady drag and lift coefficients, respectively, for the tandem cylinders for $\alpha = 0.431$ and $\beta = 0.397$. A comparison

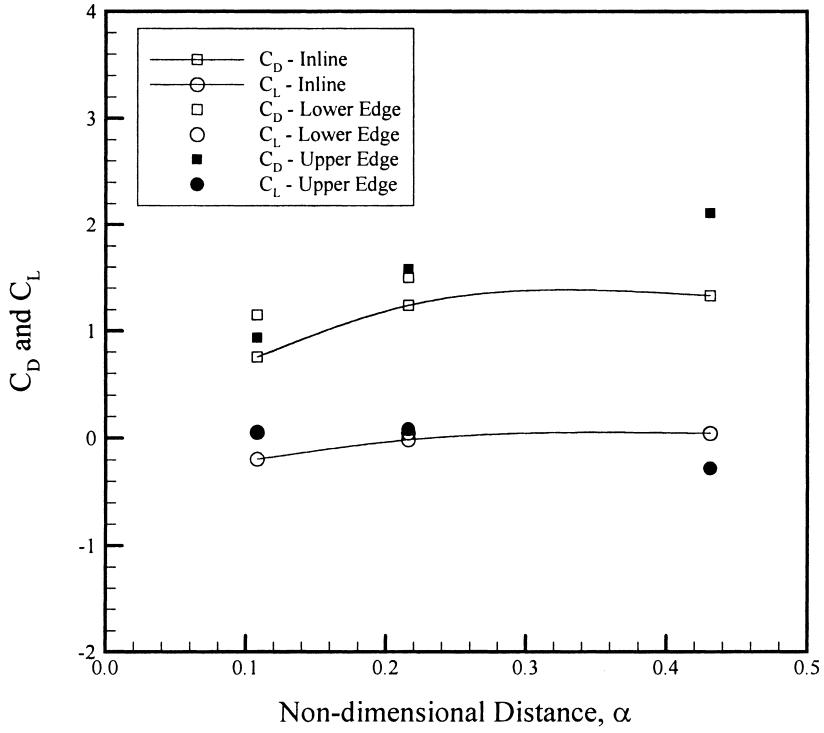

Fig. 10. C_D and C_L as a function of cylinder position for the inline and offset tandem cylinders.

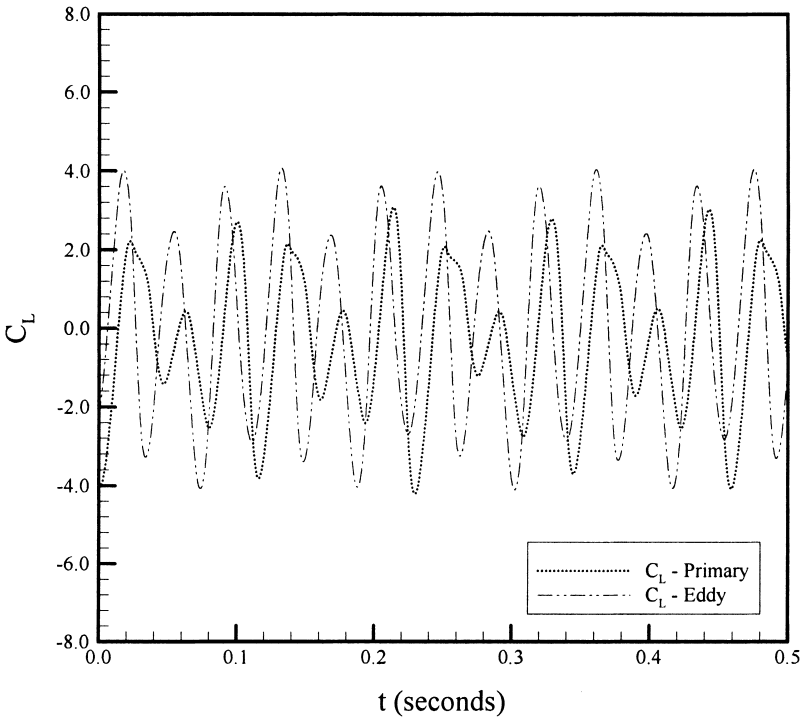

Fig. 11. Instantaneous lift coefficient traces for the heated and eddy-promoting cylinders ($\alpha = 0.431$, $\beta = 0.397$).

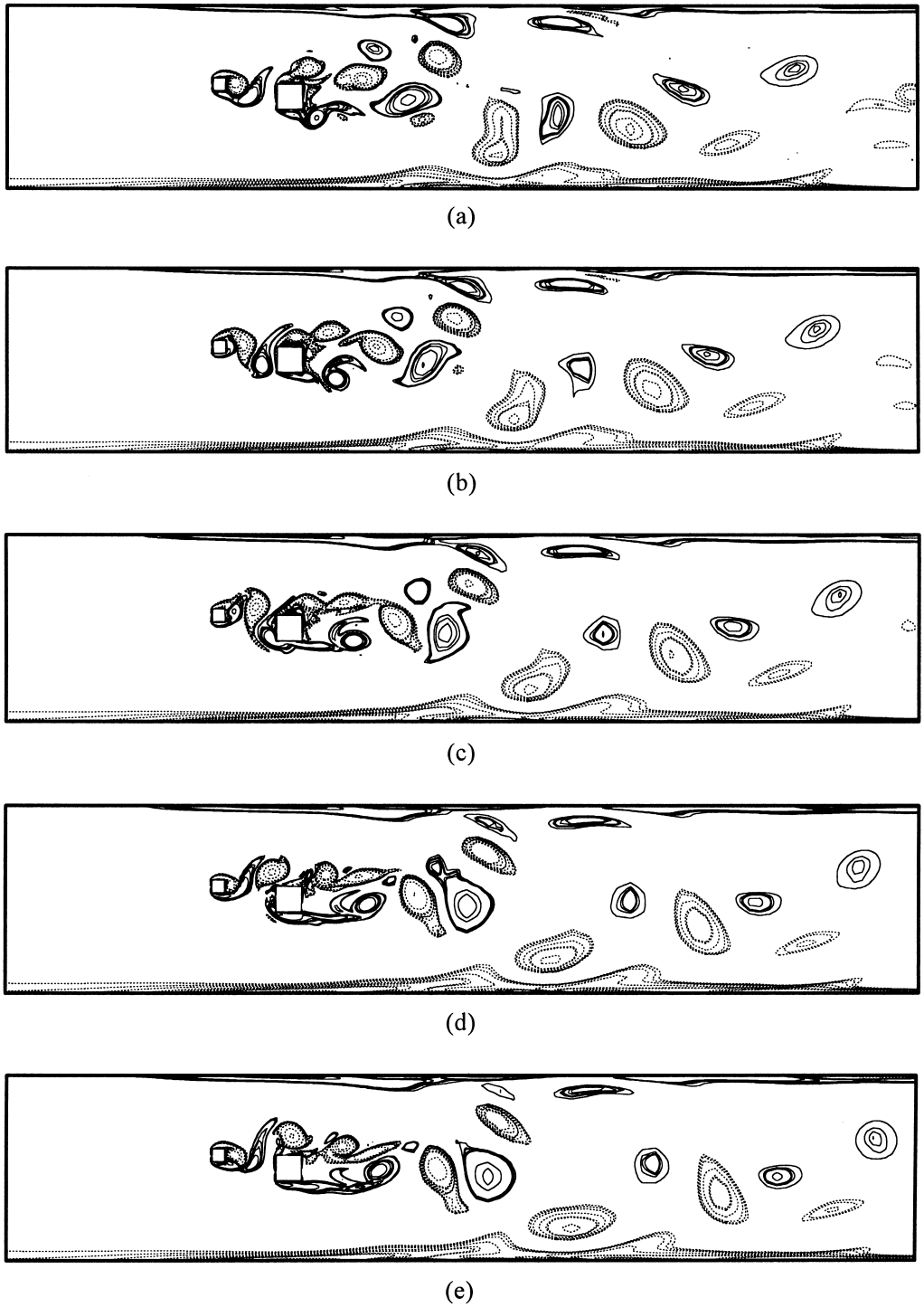

Fig. 12. Time series of vorticity for offset tandem cylinders ($\alpha = 0.431$, $\beta = 0.397$); (a) $\tau = 0$, (b) $\tau = 0.25$, (c) $\tau = 0.50$, (d) $\tau = 0.75$, (e) $\tau = 1.0$.

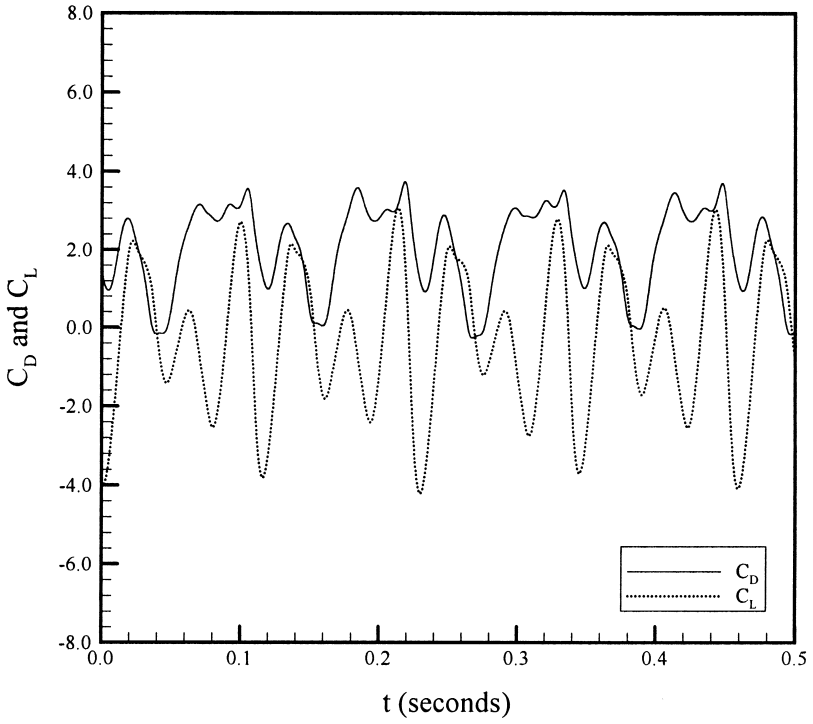

Fig. 13. Instantaneous drag and lift coefficients for the offset cylinders ($\alpha = 0.431$, $\beta = 0.397$).

of Figs. 3 and 12 shows a marked contrast in the characteristics of the fluid flow in the channel downstream of the cylinders. The displacement of the eddy cylinder from an inline to a staggered arrangement causes the vortex shedding to change from a simple steady periodic motion to a complex periodic motion. For the inline tandem cylinders, the shed vortices are convected along a narrow path with minimal interaction with the channel wall boundary layers. However, the vortices significantly distort the boundary layers within a few cylinder diameters downstream when the cylinders are staggered. The five time-series snapshots in Fig. 12 represent one vortex-shedding event. A vortex-shedding event is characterized by the process of having a pair of vortices shed from each side of the cylinder. Fig. 13 shows that three vortex-shedding events are required to form one complete repeating cycle. Although quite complicated, the nonlinear interaction between the vortices shed from the heated cylinder and those shed from the eddy promoter are not chaotic but very periodic. The time-series snapshots presented in Figs. 3, 5 and 14 also represent one vortex-shedding event and not necessarily one complete cycle. Figs. 14 and 15 show time-series snapshots and temporal traces of the unsteady drag and lift coefficients, respectively, for the tandem cylinders for $\alpha = 0.108$ and $\beta = 0.0734$. A comparison of Figs. 5 and 14 reveals that the inline upstream eddy cylinder promotes a stronger jet between the primary cylinder and the upper channel wall. This strong jet increases the strength of the vortex shed from the bottom surface of the main cylinder. This is not observed in Fig. 14 where the vortices are weaker. The offset eddy promoter effectively diverts the flow away from the narrow passage between the wall and the upper surface of the primary cylinder. In Fig. 15, the occurrence of low frequency "beating" (i.e. periodic amplitude modulation) can be observed from amplitude variations in the temporal traces of the drag and lift coefficients. This low frequency variation in the amplitude of the drag and lift traces was also observed for a single cylinder placed near a wall [8].

9. Conclusions

The characteristics of the fluid flow and heat transfer due to an inline and offset tandem pair of cylinders has been investigated numerically. The cylinders were located at several positions in a channel with a hydrodynamically fully-developed inlet velocity profile. All the numerical simulations were performed at a Rey-

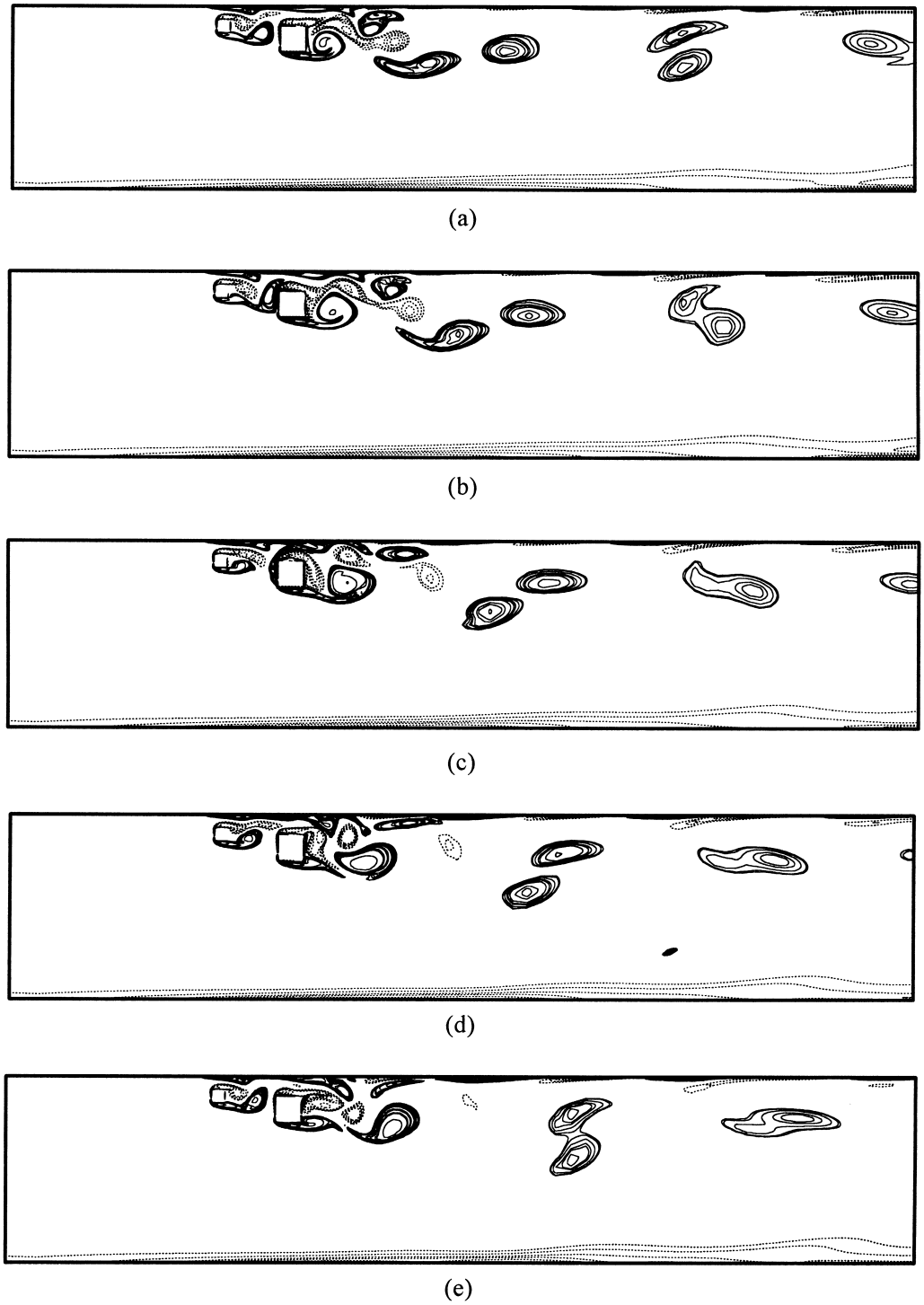

Fig. 14. Time series of vorticity for offset tandem cylinders ($\alpha = 0.108$, $\beta = 0.0734$): (a) $\tau = 0$, (b) $\tau = 0.25$, (c) $\tau = 0.50$, (d) $\tau = 0.75$, (e) $\tau = 1.0$.

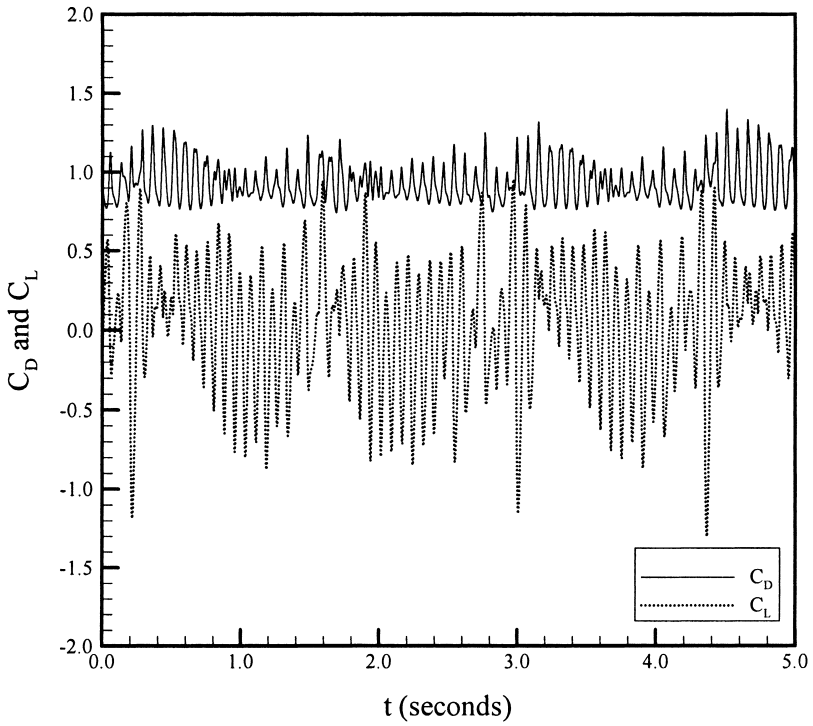

Fig. 15. Instantaneous drag and lift coefficients for the offset cylinders ($\alpha = 0.108$, $\beta = 0.0734$).

nolds number of 500 based on the larger heated cylinder. The alignment of the tandem cylinders and their location in the channel determined whether a simple, steady periodic or a complex periodic vortex shedding occurred downstream of the cylinders. The complexity of the unsteady flow field produced by the cylinder configurations can be clearly demonstrated by numerical visualization. A summary of the results obtained in this study is given below.

1. As the inline or offset tandem pair of cylinders is positioned closer to a channel wall, both the overall heat transfer and drag are reduced. The dominant mechanism seems to be the reduced velocity near the channel wall because of the parabolic velocity distribution.
2. Offsetting the eddy-promoter causes a significant reduction in the heat transfer and a large increase in the drag for the channel-centered heated cylinder as compared to an inline eddy promoter. It is found to slightly reduce the overall heat transfer and increase the drag from the downstream heated cylinder for the other two transverse locations. This is contrary to the negligible effects on the drag and heat transfer found in previous studies using a uniform inlet velocity profile.
3. For the offset eddy-promoter, little difference is found between placement of the promoter on the upper or lower edges of the heated cylinder.
4. The Strouhal number from the primary cylinder is dependent on the placement of the smaller upstream eddy-promoting cylinder. The results indicate that placement of the eddy-promoter in higher velocity fluid increases the Strouhal number.

The present study revealed pronounced differences in the unsteady behavior of an inline or offset tandem pair of cylinders in a fully-developed parabolic channel flow when compared to a channel flow with an initially uniform inlet velocity profile. The optimum placement of the eddy-promoting cylinder as a function of relevant geometrical and dynamical parameters is the subject of continuing work.

Acknowledgements

This work was initiated under the support of a National Science Foundation PYI grant to the second author, number CTS 9057465. Additional support from Raytheon/Texas Instruments through a seed grant administered by Dr. Don Price is gratefully acknowledged. The authors would like to thank Dr. Nestor Queipo for his assistance during the early stages of this research.

References

[1] R.J. Moffat, A. Ortega, Direct air cooling of electronic components, in: A. Bar-Cohen, A.D. Kraus (Eds.), Advances in Thermal Modeling of Electronic Components and Systems, vol. 1, Hemisphere, New York, 1988 (Chapter 3).

[2] H. Schlichting, Boundary-Layer Theory, 7th ed., McGraw-Hill, New York, 1987.

[3] G. Li, J.A.C. Humphrey, Numerical modelling of confined flow past a cylinder of square cross-section at various orientations, Int. J. Numer. Methods Fluids 20 (1995) 1215–1236.

[4] R. Tatsutani, R. Devarakonda, J.A.C. Humphrey, Unsteady flow and heat transfer for cylinder pairs in a channel, Int. J. Heat Mass Transfer 36 (1993) 3311–3328.

[5] A. Valencia, Unsteady flow and heat transfer in a channel with a built-in tandem of rectangular cylinders, Numer. Heat Transfer, Part A 29 (1996) 613–623.

[6] R. Devarakonda, J.A.C. Humphrey, Interactive computational–experimental methodologies in cooling of electronic components, Computer Mechanics Laboratory, Technical Report No. 92-008, University of California, Berkeley, CA, 1992.

[7] R. Devarakonda, Experimental and numerical investigation of unsteady bluff body flows, Ph.D. Dissertation, University of California at Berkeley, Berkeley, CA, 1994.

[8] J.L. Rosales, A. Ortega, J.A.C. Humphrey, A numerical investigation of the convective heat transfer in unsteady laminar flow past a single and tandem pair of square cylinders in a channel, Numer. Heat Transfer, Part A, in press (2000).

[9] N.V. Queipo, On the optimum placement of heat sources in an enclosure based on adaptive search and machine learning, Ph.D. Dissertation, University of California at Berkeley, Berkeley, CA, 1995.

[10] N.V. Queipo, J.A.C. Humphrey, A. Ortega, Multiobjective optimal placement of convectively cooled electronic components on printed wiring boards, IEEE Trans. Components, Packaging, and Manufacturing Technology, Part A (1998) 142–153.

[11] J.L. Rosales, A numerical investigation of the convective heat transfer in confined channel flow past cylinders of square cross-section, Ph.D. Dissertation, University of Arizona, Tucson, 1999.

[12] S.V. Patankar, Numerical Heat Transfer and Fluid Flow, Hemisphere, McGraw-Hill, New York, 1980.

[13] G.E. Schneider, M. Zedan, A modified strongly implicit procedure for the numerical solution of field problems, Numer. Heat Transfer 4 (1981) 1–19.